# Dynamics and biomedical application of novel superparamagnetic helical nanorobots

Suvra S. Laha[1#], Debayan Dasgupta[1#], Reshma V. R.[2], Ramray Bhat[3], Deepak K. Saini[3], Ambarish Ghosh[1,4*]

[1]Centre for Nano Science and Engineering, Indian Institute of Science, Bangalore, 560012 India.
[2]Centre For BioSystems Science and Engineering, Indian Institute of Science, Bangalore 560012, India.
[3]Department of Molecular Reproduction, Development and Genetics, Indian Institute of Science, Bangalore, 560012 India.
[4]Department of Physics, Indian Institute of Science, Bangalore 560012, India.

[#]These authors contribute equally to this work.

*Corresponding author: *ambarish@iisc.ac.in*

**Keywords:** superparamagnetism, nanorobots, magnetic hyperthermia

## Abstract

The magnetic nanorobots, primarily composed of ferromagnetic materials, have been extensively investigated for their potential applications in cellular diagnostics and therapy. However, because of the substantial magnetic remanence exhibited by ferromagnetic materials, the magnetic stability of these nanorobots is a matter of serious concern. Here, we have designed and developed superparamagnetic iron oxide nanoparticles'(SPIONs) functionalized nanorobots (SPIONs-NR), a unique system that is highly stable against magnetic agglomeration. This kind of arrangement of random magnetic moments adhering to the nanorobot's surface is relatively new and has not been previously explored in terms of fundamental physics and biomedical applications. We have carefully analyzed the various dynamical aspects of these functionalized nanorobots by studying their precession angle as a function of applied frequency at different magnetic fields. Furthermore, these functionalized nanorobots can be controllably maneuvered in the extracellular matrix by the application of rotating magnetic fields of comparatively lower magnitudes (usually < 50 G) to selectively target and annihilate malignant tissues via magnetic hyperthermia-induced localized heating, and therefore, making SPIONs-NR promising candidates in modernizing advanced nanomedicine research.

Magnetic nanostructures have been largely explored and investigated because of their significant contribution in the field of nanotherapeutics[1-4]. From spherical particles to anisotropic structures, like rods, rings, cubes, etc., magnetic nanomaterials based on iron oxides have witnessed extensive applications to address major biomedical concerns[5-10]. However, there are certain limitations associated with these isolated nanostructures. It is somehow a challenging task to steer a swarm of such nanostructures to the tumor-specific site by the application of an external magnetic field. The possibility of particles getting diffused in the biological space is significantly higher, and maneuverability, in this case, is greatly compromised. Furthermore, unwanted particle aggregation in the physiological system may severely affect the normal functioning of various treatment modalities[11]. On the contrary, inspired by the flagellar motion of bacteria, magnetic nanorobots, primarily composed of ferromagnetic components like Fe**,** Fe-Co, FePt, can be safely guided to the diseased-specific site by means of rotating magnetic fields of reasonably low magnitudes, typically < 80 Gauss, which is not detrimental to healthy tissues[12-16]. The nanorobots are widely studied and much appreciated for their controlled manipulation and precise delivery of payloads in the physiological space[14, 17-19]. These tiny magnetic robots are capable of controlled navigation through low Reynolds number fluid (where viscous forces dominate over inertial forces), mimicking physiologically relevant environments like blood, urine, mucus, saliva[20-23]. Recently, the work by Pal *et al*[13] have taken a prime step forward and successfully demonstrated cellular uptake and precise manipulation of these ferromagnetic helices in the congested intracellular space, which is a significant achievement for potential utilization of these tiny robots in future theranostics. However, due to the presence of strong ferromagnetic components of iron, stability of these nanorobots against magnetic agglomeration is a matter of serious concern. Once these nanorobots come closer in the presence of an external magnetic field, it may adhere to one another *via* mutual magnetic attraction. It is quite an arduous task to separate such robots even after turning off the applied magnetic field, primarily because of the relatively higher magnetic remanence exhibited by metallic iron. Efforts were significantly directed to functionalize the surfaces of these ferromagnetic helices with zinc ferrite coatings, which simultaneously reports much improved stability and hyperthermia efficacy[24]. However, the possibility of a futuristic therapeutic vehicle exhibiting controlled manipulation is severely compromised, particularly because of the coating thickness which is non-uniform and exceedingly higher (~700-950 nm). Consequently, comes the need for a sophisticated nano-vehicle which must be highly directional, can transport substantial cargo and perform the desired action at the diseased-specific site. In the present work, we have successfully fabricated

SPIONs functionalized nanorobots (abbreviated as SPIONs-NRs), exhibiting excellent stability against magnetic clustering or agglomeration. Additionally, we have analyzed the various dynamical aspects of these nanorobots which holds immense potential as the next-generation therapeutic vehicle, demonstrating controlled maneuverability in the extracellular matrix (ECM) at relatively lower magnetic fields (<50 Gauss), accompanied by targeted release of hyperthermia-induced local heat at the single-cell resolution. The 2.8-3.0 μm sized silica helices were fabricated using the standard glancing angle deposition technique (details available in Supporting Information). The helices were then functionalized with SPIONs using the microwave synthesizer (details available in Supporting Information). This system of nanorobots, with a random arrangement of magnetic moments on the silica surface is relatively new and carries great significance from the standpoint of analyzing the underlying physics of such a complex magnetic spin configuration. Previously, coating of thin films of ferrites were mostly conducted on these helices using microwave synthesizer, however, covering the entire silica surface with nanoparticles was never realized [24]. The primary purpose for coating these helices with iron oxide nanoparticles is to render their surfaces superparamagnetic, a critical factor to ensure their stability against magnetic agglomeration. Furthermore, the SPIONs (US Food and Drug Administration approved nanomaterials for clinical applications) are reported to be highly biocompatible, exhibit relatively higher value of saturation magnetization and specific absorption rate (SAR)[25-27], which are essential prerequisites for advanced biomedical applications. The nanoparticles get firmly coated on the surface of a SPIONs-NR, as distinctly evident from **Figure 1A**. The X-ray diffraction (XRD) in the inset clearly indicates the formation of iron oxide, characterized by the most intense (311) peak[26]. The signature of (111) peak of gold is due its presence in the substrate. The thickness of the robots, or precisely, the width of the several layers of iron oxide nanoparticles on the silica helix, reported here is nearly halved (~300–550 nm) as compared to those stabilized by zinc-ferrite coating[24]. Considering the average nanoparticle size to be somewhere around 12 nm, we can hypothesize, that nearly 25 to 40 layers of such particles are typically adhering to the surface of the silica helices. In this case, the magnetic component, unlike reported for other ferromagnetic helices (both inline and laid down helices)[13, 20, 24, 28-29], decorates the entire silica surface, making it a unique system to explore interesting dynamical properties as well as biomedical applications. A magnified image of the nanoparticle distribution on the silica surface is clearly shown in **Figures 1B, 1C**. Few layers of nanoparticles of size ranging between 11-13 nm can be seen firmly resting on the surfaces of the silica helices (**Figure 1C**). A careful investigation using

high-resolution transmission electron microscopy (HR-TEM) could even detect the presence of isolated crystalline nanoparticles impregnated on the silica surface, characterized by well-defined atomic planes corresponding to $Fe_3O_4$ (**Figure 1D**). The mechanism of bonding of SPIONs to the silica surface is somewhat interesting, and may be attributed to the formation of stable Fe-O-$Si(OH)_3$ bonds as described elsewhere[30]. The Scanning transmission electron microscope (STEM) mode of imaging has been implemented to quantitatively evaluate the elemental composition of the helices. The STEM image of a typical SPIONs-NR depicting the presence of silicon (Si: Blue) and iron (Fe: Red) is shown in **Figure 1E**. The relative concentration of silicon and iron expressed in *% wt.*, is understood by the mass fraction, expressed as, Si**:**Fe ~ 60:40. The duration of *hold time* (microwave time) and the quantity of nanoparticles used for the microwave coating are the two primary factors which decides the nanoparticle thickness on the silica helices (for details see Supporting Information). The number of nanoparticle stacks adhering to the silica surface can easily be tuned by altering the microwave heating time and the concentration of the precursor nanoparticle dispersion. This is quite unique in a way as one can accordingly control the nanoparticle concentration, or in other words, the magnetic moment of these helices simply by manipulating these two parameters. The average mass fraction calculated on an ensemble of such nanorobots is approximately, Si**:**Fe ~ 65:35. It is supposed that for an ideal system of superparamagnetic nanoparticles (the magnetic remanence of these 12-13 nm sized single-domain nanoparticles boils down to near-zero when the external field is turned off), clustering or aggregation can easily be avoided. However, this situation remains mostly unachieved under practical conditions and the nanoparticles do form agglomerates which could affect the hyperthermia heating efficiency to a considerable extent. On the contrary, our SPIONs-NR, loaded with tens of thousands of such superparamagnetic nanoparticles, demonstrate excellent stability primarily against magnetic clumping or agglomeration as illustrated in **Figure 1F**. In the presence of an externally applied magnetic field of strength of 50 Gauss, the nanorobots were initially driven close to one another. This is made possible primarily because the first cut-off frequencies ($\Omega_1$) of the two robots are different ($\Omega_1$ is that critical frequency at which a nanorobot migrates to precession from a tumbling motion)[29], and therefore, one of them was exhibiting translational motion (arising from the rotation-transitional coupling due to the inherent chirality of these nanorobots) while the other one was subjected to tumbling at a particular frequency. The panels in **Figure 1F** depicts how the two robots approach each other, then got adhered to one another via mutual magnetic attraction, and were subsequently released as the field is turned off,

implying near-zero magnetic remanence exhibited by the SPIONs. This observation bears enough testimony to our claim supporting the magnetic stability of these therapeutic vehicles (Video available in Supporting Information).

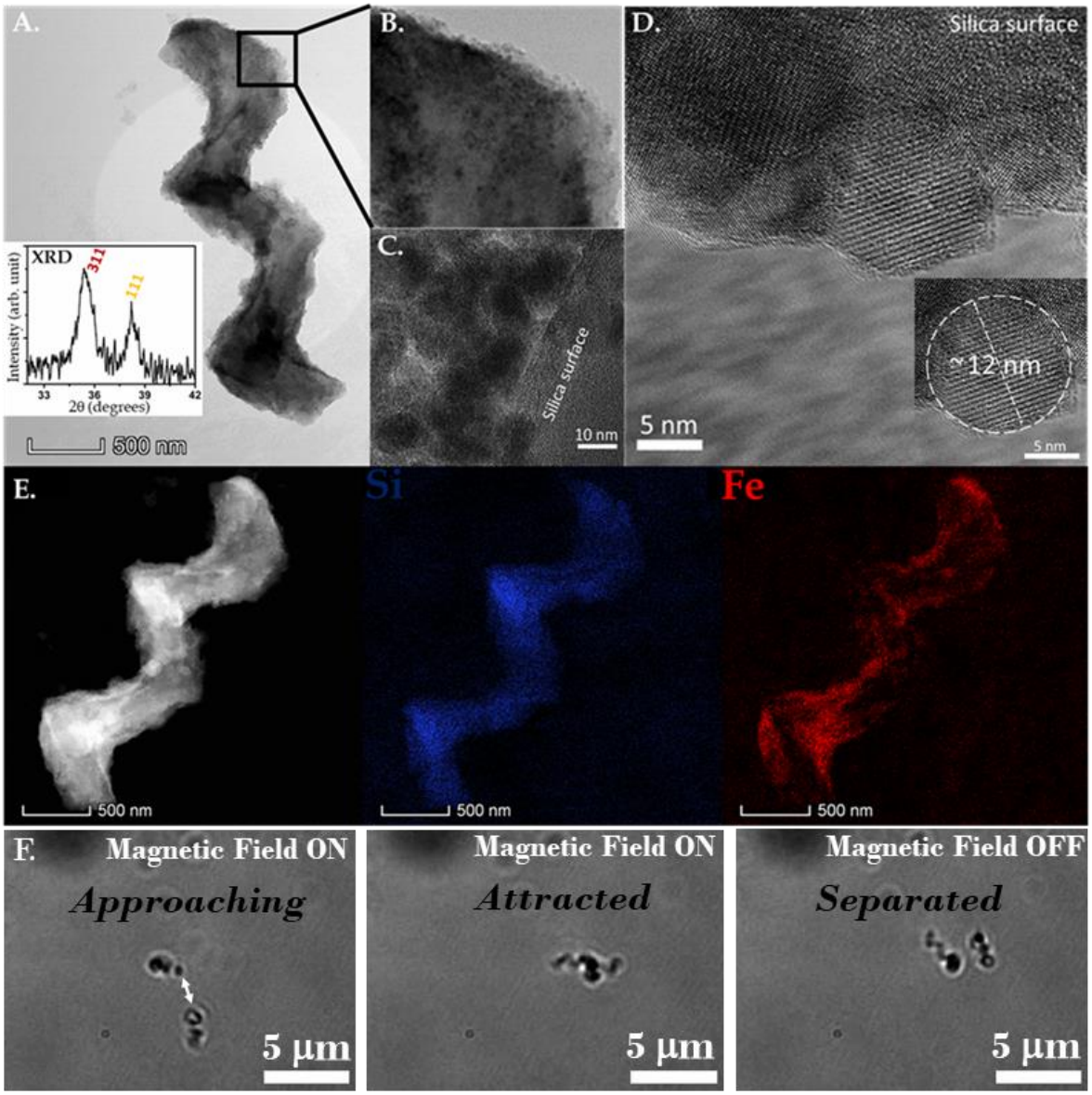


**Figure 1: Integration of SPIONs to nanorobots to form superparamagnetic therapeutic vehicles** **A.** TEM image of a SPIONs-NR of size length 2.8-3.0 µm. The inset shows the XRD of SPIONs coated nanorobots. The most intense diffraction peaks of $Fe_3O_4$ (311) and Au (111) are shown. The occurrence of (311) peak confirms coating of SPIONs onto the surfaces of these standing nanorobots *ie.* robots still on the substrate. The Au peak arises due to the presence of gold coating on the substrate or the seed layer on which these robots are grown using GLAD **B.** Magnified view depicting the distribution of $Fe_3O_4$ nanoparticles on the nanorobot's surface **C.** TEM image showing the impregnation of $Fe_3O_4$ nanoparticles on the silica surface of the nanorobot **D.** High resolution TEM (HRTEM) image clearly showing crystalline $Fe_3O_4$ nanoparticles adhering to the robot's silica surface. The inset depicts one such 12 nm-sized nanoparticle with well-defined atomic planes. **E.** Scanning transmission electron microscope (STEM) image of a SPIONs -NR depicting the presence of Si (Blue) and Fe (Red). The mass fraction of Si**:**Fe is nearly 60**:**40. The average mass fraction of Si**:**Fe on ten such nanorobots is

approximately 65**:**35 **F.** The images confirming the superparamagnetic behavior exhibited by SPIONs-NR. In the presence of a magnetic field of strength 50 Gauss, initially, they approach each other, then got stuck due to mutual attraction and finally released once the field is turned off. Please refer to the Supporting information for the detailed video.

Interestingly, these nanorobots with 10-12 nm-sized iron oxide nanoparticles covering the entire silica surfaces display novel dynamical behavior. This kind of a unique arrangement, where a helix is decorated with superparamagnetic particles have not been previously studied. Morozov *et al.* [31] have developed a theory for superparamagnetic chiral nanorobots, where they have explained the experimentally observed regimes with theoretically calculated dynamic orientation. However, in the case of SPIONs-NR, the experimental observations diverge from the theory established by Morozov *et al.* regardless of the superparamagnetic nature of our nanorobots. This departure from theory arises possibly due to the non-zero dipole-dipole interaction existing between neighboring particles, which has not been considered earlier. Interestingly, the dipolar interaction gives rise to a ferromagnetic-like behavior in the nanorobot dynamics. The **Figure 2A** represents the schematic of a typical nanorobot. The dynamical measurements of SPIONs-NR were conducted in water: glycerol mixture (1:1; v/v) and the corresponding results are shown in **Figure 2B.** The dynamics of the nanorobots was imaged and analyzed to estimate the precession angle $\alpha_p$. The data are plotted on the theoretical formula $\alpha_p = \mathbf{sin^{-1}(\Omega_1/\Omega_B)}$, where $\Omega_1$ signifies the experimentally calculated frequency corresponding to tumbling-precession transition and $\Omega_B$ is the actuation frequency. The detailed expression of the precession angle is shown in **Figure 2A**, where $m$ and $\theta_m$ represents the magnetic moment of the nanorobot and the angle of magnetization respectively, $B$ denotes applied magnetic field strength, $\eta$ corresponds to the effective viscosity of the medium and $f_s$ is a geometrical factor associated with the drag coefficient. The precession angle of SPION-NRs typically follows a sine-inverse curve, identical to the ferromagnetic nanorobots[29, 32]. The plot depicts superparamagnetic nanoparticles adhering to the helical surface imparts interesting dynamical properties which reflects ferromagnetic-like behavior. The experiment was performed at five different magnetic field intensities (35 G, 40 G, 50G, 60G and 70 G). This deviation in the dynamical behavior of superparamagnetic nanorobots from the established theory, can possibly be explained using simulation studies incorporating the existence of dipolar interactions between the nanoparticles.

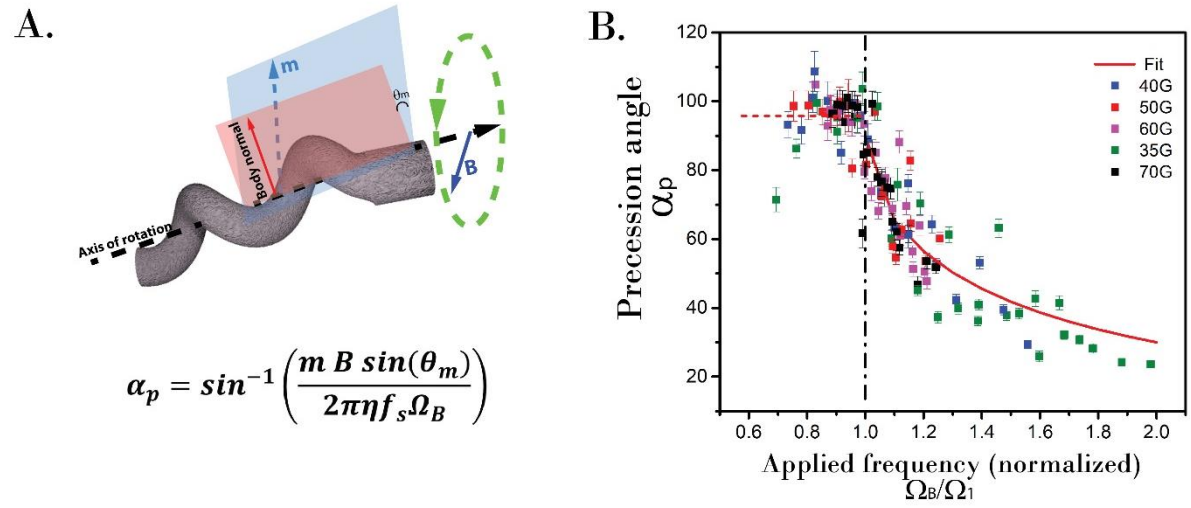


**Figure 2. Dynamical properties of superparamagnetic helical nanorobots. A.** Schematic of a typical nanorobot along with the expression of the precession angle $\alpha_p$ **B.** Precession angle *vs* normalized applied frequency. The experiment was performed at five different magnetic field intensities.

To further explore the possibility of these nanorobots in advanced biomedical applications, we have carefully probed their magnetic hyperthermic abilities. In a typical magnetic hyperthermia procedure, the nanoparticles are directly injected to the malignant tissues following which they are exposed to a high frequency alternating magnetic field. The nanoparticles absorb the magnetic energy and generate significant thermal stress in the micro-environment of the affected tissues which is sufficient to trigger major cellular dysfunctions[33]. The schematic in **Figure 3A** illustrates the experimental protocol adopted for our *in-vitro* magnetic hyperthermia studies involving human breast cancer (MDA-MB-231) cell lines and SPIONs-NR as the local heat-generating sources. The MDA-MB-231 cells were suspended between two layers of Matrigel of varying concentrations (sandwich-like arrangement in a 35 mm glass bottom dish representing a quasi-2D layer of cells, **Figure 3A**, details available in Supporting Information) to somewhat mimic the physiological environment. The SPIONs-NR were then carefully injected and magnetically steered through the extracellular matrix (ECM) (**Figure 3B**, video available in Supporting Information). The nanorobots were maneuvered in the ECM using magnetic field of magnitude 40 Gauss rotating at a frequency of 3-4 Hz. The magnitude of the rotating field is relatively lower, as a much higher field close to 80-100 Gauss could result in excessive Joule heating of our triaxial Helmholtz coil (experimental set-up). This is primarily achieved as the magnetic moments of these nanorobots, decorated with iron oxide nanoparticles, are substantially higher, eventually allowing a field as low as 40 Gauss to

drive them with high precision in the ECM. In this case, the cancer cells were incubated for a period of ~24 hrs. The period of incubation plays a significant role, as a ~24h incubation, prevents significant secretion of sialic acid by the cancer cells in the tumor microenvironment. As reported by Dasgupta *et al* [28], ~72 hrs incubation substantially remodels the tumor extracellular matrix in terms of extensive sialic acid linkages, which restricts nanorobots to get adhered to the cancer-proximal ECM. The glass bottom dish containing cancer cells incubated with SPIONs-NR was then subjected to 1000 seconds of magnetic hyperthermia under a high-frequency (*f*=220 kHz) alternating magnetic field of amplitude ~30 kA/m (details available in Supporting Information). The presence of highly viscous Matrigel promotes rigid anchoring of SPIONs-NR with the cancer cell's surface. To quantitatively assess post-hyperthermia cell viability, the MDA-MB-231 cells were stained with a red fluorescent dye, namely, propidium iodide or PI. PI primarily penetrates and binds to the DNA components, once the cell membrane is ruptured. It fluoresces red, implying cell death, upon excitation with a green illumination source. As it can be observed from the high-resolution microscopic images in **Figure 3C**, the areas or regions of the cell, in close association with SPIONs-NR (indicated by arrows) fluoresced red, which is a clear indication of cell death *via* magnetic hyperthermia induced heating. To obtain a statistical interpretation of post-hyperthermia cell viability, n=3 representative hyperthermia experiments (t=1000s, *f*=220kHz, H ~30 kA/m) were conducted and the subsequent results are demonstrated in **Figure 3D**. From the histogram data (**Figure 3D**), it is clearly observed that nearly 75% of the cancer cells in physical association with SPIONs-NR have succumbed to hyperthermia induced heating. However, only ~20% of the cells suffer death even in the absence of SPIONs-NR. It is to be noted that very few nanorobots adhered to the cell surface, because there is a few order-of-magnitude difference between the number of cells and the injected robots. We proposed that hyperthermia-induced local heat emanating from SPIONs-NR, has substantially rupture the membrane causing a leakage of cell's DNA components, and hence the pronounced PI fluorescence. During magnetic nanoparticle hyperthermia, the flipping of magnetic moments (Néel relaxation) and frictional contributions triggering physical rotation of the particle (Brownian relaxation) are the two most prominent nanomagnetic phenomena that accounts for substantial heat generation[33]. The Néel relaxation time ($\tau_N$) depends on the magneto-crystalline anisotropy energy barrier ($E_A$) and is expressed using the Arrhenius relation, $\tau_N = \tau_0 \exp(E_A/k_BT)$, where $k_B$ is the Boltzmann's constant, $T$ is the temperature and $\tau_0$ is the attempt time characteristic of the material ($10^{-13}$–$10^{-9}$s)[26, 34-36]. However, the Brownian relaxation mechanism is much controlled by the

viscosity of the medium ($\eta$) in which the nanoparticles are suspended and is given by $\tau_B = \frac{4\pi\eta r_h^3}{k_B T}$, where $r_h$ is the average hydrodynamic radius of the nanoparticle ensemble. In the presence of both the relaxation processes, the effective relaxation time can be expressed as $\tau_{eff.} = \frac{\tau_N \tau_B}{\tau_N + \tau_B}$[25]. For a typical 12-13 nm sized SPION, $\tau_B$ and $\tau_N$ are in the order of ~$10^{-5}$s and ~$10^{-8}$s respectively, therefore, the magnetic spin moment reversal or the Néel relaxation is the principal contributing factor for localized heat production in magnetic nanoparticle hyperthermia[25]. In this specific system of nanorobots, the superparamagnetic nanoparticles are tightly bound to the silica surfaces. Consequently, the heat loss *via* Brownian relaxation is strictly restricted in this case. The mechanism of heat generation comes primarily from the intrinsic Néel relaxation as well as from the *ac* magnetic hysteresis losses, as the particle spins fail to follow the high frequency (~220 kHz) of the alternating magnetic field[33]. In this case, the red fluorescence response primarily arises when the DNA components ooze out and bind to the PI following the rupture of the cell membrane. The mechanism of cell annihilation *via* magnetic nanoparticle hyperthermia is still debatable, and there are reports attributing hyperthermia induced cell death to both *apoptosis* (programmed cell death) and *necrosis* (unprogrammed cell death)[37-38]. There are various factors, particularly, the concentration of nanoparticles, nature of ECM, local heating efficacy etc[38]. which practically decides the nature of cell death triggered by magnetic nanoparticle hyperthermia. However, in this case, we hypothesize, that in the presence of a high frequency alternating magnetic field, the iron oxide nanoparticles adhering to the nanobots trigger sudden heat shocks or imparts highly localized thermal stress, creating sub-local damages in the cell membrane (leading to membrane rupture), which possibly manifests in a necrosis-induced cell death.

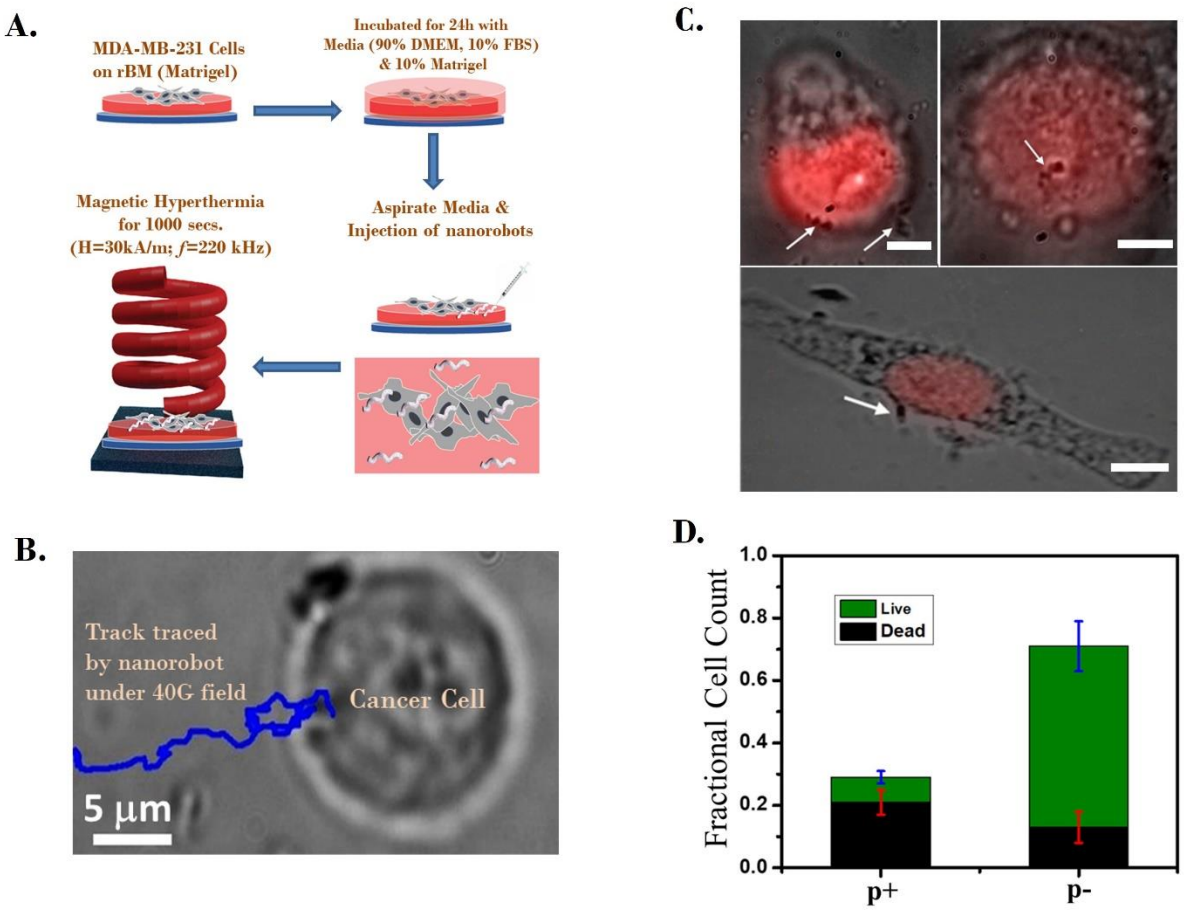


**Figure 3: Targeted delivery of SPIONs-NR in ECM & therapeutic efficiency**. **A.** Schematic showing the cell culture protocol involving MDA-MB-231 cells, injection of nanorobots in the ECM and subsequent performance of magnetic hyperthermia for t= 1000 secs at H~ 30kA/m; *f* = 220 kHz **B.** The blue line depicting the track traversed by a nanorobot when magnetically steered towards a cancer cell under the presence of a magnetic field of amplitude 40 Gauss **C.** PI-stained MDA-MB-231 cells (post-hyperthermia). The red fluorescent PI signal indicating cell death when the cell is in physical contact with SPIONs-NR (pointed by white arrows). The scale bars represent 5 µm. **D.** Fractional cell count for n=3 representative experiments depicting cell live/dead in presence (p+) and absence (p-) of nanorobots (post-hyperthermia).

We have successfully designed and developed SPIONs' functionalized nanorobots, a unique system, comprising of 10-12 nm-sized iron oxide nanoparticles firmly adhered to the surfaces of the 2.8-3.0 µm long silica helices. The stable coating of iron oxide particles over the entire silica surfaces was successfully achieved using the microwave synthesizer. SPIONs-NR are reported to be highly stable against magnetic agglomeration, primarily because of the near zero remanence exhibited by the superparamagnetic particles covering their surfaces. The random arrangement of magnetic spins on the helical surface creates interesting dynamical properties of these functionalized nanorobots. The precession angle vs applied frequency analysis reveals that individual superparamagnetic nanoparticles adhering to the silica helix collectively impart

dynamical properties which corresponds to a ferromagnetic-like behavior. Finally, these iron oxide functionalized robots prove to be a significant nano-vehicle, which are controllably maneuvered in the ECM at comparatively lower fields (<50 Gauss), for delivering magnetic hyperthermia-induced local heat at the single-cell resolution, possibly leading to cell death *via* necrosis. The chemistry of conjugating iron oxide particles with cancer drug molecules, particularly, doxorubicin, is well established. In future, SPIONs-NR can be functionalized with cancer drugs to bring about a synergistic approach of cell killing via magnetic hyperthermia induced localized heating.

**Acknowledgements**

SSL acknowledges SERB-NPDF and CSIR-SRA (Scientists' Pool Scheme) for financial support. All the authors further acknowledge the Micro Nano Characterization Facility (MNCF) at Centre for Nano Science and Engineering (CeNSE), IISc Bangalore.

## References


1. Pankhurst, Q. A.; Connolly, J.; Jones, S. K.; Dobson, J., Applications of magnetic nanoparticles in biomedicine. *Journal of physics D: Applied physics* **2003,** *36* (13), R167.
2. Leslie-Pelecky, D. L.; Rieke, R. D., Magnetic properties of nanostructured materials. *Chemistry of materials* **1996,** *8* (8), 1770-1783.
3. McBain, S. C.; Yiu, H. H.; Dobson, J., Magnetic nanoparticles for gene and drug delivery. *International journal of nanomedicine* **2008,** *3* (2), 169.
4. Laha, S. S.; Thorat, N. D.; Singh, G.; Sathish, C.; Yi, J.; Dixit, A.; Vinu, A., Rare-Earth Doped Iron Oxide Nanostructures for Cancer Theranostics: Magnetic Hyperthermia and Magnetic Resonance Imaging. *Small* **2022,** *18* (11), 2104855.
5. Arachchige, M. P.; Laha, S. S.; Naik, A. R.; Lewis, K. T.; Naik, R.; Jena, B. P., Functionalized nanoparticles enable tracking the rapid entry and release of doxorubicin in human pancreatic cancer cells. *Micron* **2017,** *92*, 25-31.
6. Das, R.; Alonso, J.; Nemati Porshokouh, Z.; Kalappattil, V.; Torres, D.; Phan, M.-H.; Garaio, E.; García, J. A. n.; Sanchez Llamazares, J. L.; Srikanth, H., Tunable high aspect ratio iron oxide nanorods for enhanced hyperthermia. *The Journal of Physical Chemistry C* **2016,** *120* (18), 10086-10093.
7. Liu, X.; Zheng, J.; Sun, W.; Zhao, X.; Li, Y.; Gong, N.; Wang, Y.; Ma, X.; Zhang, T.; Zhao, L.-Y., Ferrimagnetic vortex nanoring-mediated mild magnetic hyperthermia imparts potent immunological effect for treating cancer metastasis. *ACS nano* **2019,** *13* (8), 8811-8825.
8. Liu, X. L.; Yang, Y.; Ng, C. T.; Zhao, L. Y.; Zhang, Y.; Bay, B. H.; Fan, H. M.; Ding, J., Magnetic vortex nanorings: a new class of hyperthermia agent for highly efficient in vivo regression of tumors. *Advanced Materials* **2015,** *27* (11), 1939-1944.
9. Mai, B. T.; Balakrishnan, P. B.; Barthel, M. J.; Piccardi, F.; Niculaes, D.; Marinaro, F.; Fernandes, S.; Curcio, A.; Kakwere, H.; Autret, G., Thermoresponsive iron oxide nanocubes for an effective clinical translation of magnetic hyperthermia and heat-mediated chemotherapy. *ACS applied materials & interfaces* **2019,** *11* (6), 5727-5739.
10. Song, Y.; Li, D.; Lu, Y.; Jiang, K.; Yang, Y.; Xu, Y.; Dong, L.; Yan, X.; Ling, D.; Yang, X., Ferrimagnetic mPEG-b-PHEP copolymer micelles loaded with iron oxide nanocubes and emodin for enhanced magnetic hyperthermia–chemotherapy. *National Science Review* **2020,** *7* (4), 723-736.
11. Guibert, C.; Dupuis, V.; Peyre, V.; Fresnais, J., Hyperthermia of magnetic nanoparticles: experimental study of the role of aggregation. *The Journal of Physical Chemistry C* **2015,** *119* (50), 28148-28154.
12. Kadiri, V. M.; Günther, J.-P.; Kottapalli, S. N.; Goyal, R.; Peter, F.; Alarcón-Correa, M.; Son, K.; Barad, H.-N.; Börsch, M.; Fischer, P., Light-and magnetically actuated FePt microswimmers. *The European Physical Journal E* **2021,** *44* (6), 1-11.
13. Pal, M.; Somalwar, N.; Singh, A.; Bhat, R.; Eswarappa, S. M.; Saini, D. K.; Ghosh, A., Maneuverability of magnetic nanomotors inside living cells. *Advanced Materials* **2018,** *30* (22), 1800429.
14. Venugopalan, P. L.; Esteban-Fernández de Ávila, B.; Pal, M.; Ghosh, A.; Wang, J., Fantastic voyage of nanomotors into the cell. *ACS nano* **2020,** *14* (8), 9423-9439.
15. Pal, M.; Dasgupta, D.; Somalwar, N.; Reshma, V.; Tiwari, M.; Teja, D.; Narayana, S. M.; Katke, A.; Jayshree, R.; Bhat, R., Helical nanobots as mechanical probes of intra-and extracellular environments. *Journal of Physics: Condensed Matter* **2020,** *32* (22), 224001.
16. Dasgupta, D.; Peddi MDS, S. S.; Saini, D. K.; Ghosh, A., Mobile nanobots for prevention of root canal treatment failure. *Advanced Healthcare Materials* **2022**, 2200232.
17. Ghosh, A.; Fischer, P., Controlled propulsion of artificial magnetic nanostructured propellers. *Nano letters* **2009,** *9* (6), 2243-2245.
18. Zhang, L.; Abbott, J. J.; Dong, L.; Kratochvil, B. E.; Bell, D.; Nelson, B. J., Artificial bacterial flagella: Fabrication and magnetic control. *Applied Physics Letters* **2009,** *94* (6), 064107.

19. Tottori, S.; Zhang, L.; Qiu, F.; Krawczyk, K. K.; Franco-Obregón, A.; Nelson, B. J., Magnetic helical micromachines: fabrication, controlled swimming, and cargo transport. *Advanced materials* **2012,** *24* (6), 811-816.
20. Venugopalan, P. L.; Sai, R.; Chandorkar, Y.; Basu, B.; Shivashankar, S.; Ghosh, A., Conformal cytocompatible ferrite coatings facilitate the realization of a nanovoyager in human blood. *Nano letters* **2014,** *14* (4), 1968-1975.
21. Gao, W.; Sattayasamitsathit, S.; Manesh, K. M.; Weihs, D.; Wang, J., Magnetically powered flexible metal nanowire motors. *Journal of the American Chemical Society* **2010,** *132* (41), 14403-14405.
22. Walker, D.; Käsdorf, B. T.; Jeong, H.-H.; Lieleg, O.; Fischer, P., Enzymatically active biomimetic micropropellers for the penetration of mucin gels. *Science Advances* **2015,** *1* (11), e1500501.
23. Garcia-Gradilla, V.; Orozco, J.; Sattayasamitsathit, S.; Soto, F.; Kuralay, F.; Pourazary, A.; Katzenberg, A.; Gao, W.; Shen, Y.; Wang, J., Functionalized ultrasound-propelled magnetically guided nanomotors: Toward practical biomedical applications. *ACS nano* **2013,** *7* (10), 9232-9240.
24. Venugopalan, P. L.; Jain, S.; Shivashankar, S.; Ghosh, A., Single coating of zinc ferrite renders magnetic nanomotors therapeutic and stable against agglomeration. *Nanoscale* **2018,** *10* (5), 2327-2332.
25. Nemala, H.; Thakur, J.; Naik, V.; Vaishnava, P.; Lawes, G.; Naik, R., Investigation of magnetic properties of Fe3O4 nanoparticles using temperature dependent magnetic hyperthermia in ferrofluids. *Journal of Applied Physics* **2014,** *116* (3), 034309.
26. Laha, S.; Regmi, R.; Lawes, G., Structural origin for low-temperature relaxation features in magnetic nanoparticles. *Journal of Physics D: Applied Physics* **2013,** *46* (32), 325004.
27. Cai, N.; Li, C.; Han, C.; Luo, X.; Shen, L.; Xue, Y.; Yu, F., Tailoring mechanical and antibacterial properties of chitosan/gelatin nanofiber membranes with Fe3O4 nanoparticles for potential wound dressing application. *Applied Surface Science* **2016,** *369*, 492-500.
28. Dasgupta, D.; Pally, D.; Saini, D. K.; Bhat, R.; Ghosh, A., Nanomotors sense local physicochemical heterogeneities in tumor microenvironments. *Angewandte Chemie International Edition* **2020,** *59* (52), 23690-23696.
29. Ghosh, A.; Dasgupta, D.; Pal, M.; Morozov, K. I.; Leshansky, A. M.; Ghosh, A., Helical nanomachines as mobile viscometers. *Advanced Functional Materials* **2018,** *28* (25), 1705687.
30. Taylor, P. *Interactions of silica with iron oxides: effects on oxide transformations and sorption properties*; Atomic Energy of Canada Ltd.: 1995.
31. Morozov, K. I.; Leshansky, A. M., Dynamics and polarization of superparamagnetic chiral nanomotors in a rotating magnetic field. *Nanoscale* **2014,** *6* (20), 12142-12150.
32. Ghosh, A.; Mandal, P.; Karmakar, S.; Ghosh, A., Analytical theory and stability analysis of an elongated nanoscale object under external torque. *Physical Chemistry Chemical Physics* **2013,** *15* (26), 10817-10823.
33. Telling, N., High-Frequency Magnetic Response and Hyperthermia From Nanoparticles in Cellular Environments. In *Nanomaterials for Magnetic and Optical Hyperthermia Applications*, Elsevier: 2019; pp 173-197.
34. Laha, S.; Tackett, R.; Lawes, G., Interactions in γ-Fe2O3 and Fe3O4 nanoparticle systems. *Physica B: Condensed Matter* **2014,** *448*, 69-72.
35. Laha, S. S.; Abdelhamid, E.; Arachchige, M. P.; Kumar, A.; Dixit, A., Ferroic ordering and charge-spin-lattice order coupling in Gd-doped Fe3O4 nanoparticles relaxor multiferroic system. *Journal of the American Ceramic Society* **2017,** *100* (4), 1534-1541.
36. Abdelhamid, E.; Laha, S. S.; Dixit, A.; Nazri, G. A.; Jayakumar, O. D.; Nadgorny, B., Exchange Bias Enhancement and Magnetic Proximity Effect in FeVO4-Fe3O4 Nanoparticles. *Journal of Electronic Materials* **2019,** *48* (5), 3297-3303.
37. Ito, A.; Honda, H.; Kobayashi, T., Cancer immunotherapy based on intracellular hyperthermia using magnetite nanoparticles: a novel concept of “heat-controlled necrosis” with heat shock protein expression. *Cancer Immunology, Immunotherapy* **2006,** *55* (3), 320-328.

38. Beola, L.; Asín, L.; Fratila, R. M.; Herrero, V.; De La Fuente, J. M.; Grazú, V.; Gutiérrez, L., Dual role of magnetic nanoparticles as intracellular hotspots and extracellular matrix disruptors triggered by magnetic hyperthermia in 3D cell culture models. *ACS applied materials & interfaces* **2018,** *10* (51), 44301-44313.